Erschienen in: Energy Procedia ; 27 (2012). - S. 227-233

Vailable online at www.sciencedirect.com

SciVerse ScienceDirect

Energy Procedia 27 (2012) 227 – 233

Energy Procedia

SiliconPV: 3-5 April 2012, Leuven, Belgium

Solar cell improvement by using a multi busbar design as front electrode

S. Braun*, G. Micard, G. Hahn

University of Konstanz, Department of Physics, P.O. Box X916, 78457 Konstanz, Germany

Abstract

The demand for low-priced solar cells with higher efficiencies becomes more necessary to reach grid parity. An optimized solar cell design which uses the same equipment as state of the art solar cells could be easily implemented into solar industry. In this paper an approach for a front side design is discussed, using more busbars than the widely used three busbar design for the solar cell front electrode. A simulation program based on the two-diode model was used summing up the series resistances of each contributor in a module optimizing the number and geometry of wires needed. The simulations reveal that the advantages of the multi busbar design originate from a reduction of effective finger length, opening up new possibilities for the cell design. It is demonstrated that the multi busbar solar cell design can increase the module efficiency by $0.5\%_{abs}$ and a reduction in the consumption of silver of over 89% can be achieved by using seed and plate techniques. A significant surplus in short circuit current can be realized by using round wires.

Keywords: Multi Busbar Design; Ag/Cost Reduction; Interconnected Solar Cells

1. Introduction

The starting point of the investigation was an approach to increase the module efficiency by changing the solar cell front grid design. Therefore, not only the solar cell efficiency but also the interconnected structure has to be assessed. As front electrode a multi busbar design was chosen. Hereby the busbars were exchanged by multiple wires which are connected to the perpendicularly orientated finger grid [1]. An additional tabbing is not necessary for that kind of cell design. A big contributor to the loss in

* Corresponding author. Tel.: +49 7531 882082; fax: +49 7531 883895
E-mail address: stefan.braun@uni-konstanz.de

doi:10.1016/j.egypro.2012.07.056

efficiency in a module is the additional series resistance originating from stringing of the solar cells. Instead of using a simplified model for the optimization on cell level [2], the two-diode model was used also taking into account shading of the front grid and additional resistances under interconnected conditions. The series resistance contribution of the interconnected back side was simulated using PDE solvers. Also, a comparison of a screen printed and a plated metallization was performed taking into account the amount of metal necessary for sufficient grid line conductivity. The results of the simulation are compared with a state of the art three busbar solar cell design.

2. The Simulation

To simulate the IV characteristics of a solar cell the two-diode model [3] is used. Equation (1) with voltage U, current density j, photo-generated current density j_{ph}, series resistance R_s, shunt resistance R_p, temperature T, Boltzmann constant k_B, saturation current densities of the two diodes j_{01} and j_{02} and ideality factors n_1 and n_2 has to be solved iteratively:

$$j(U) = -j_{ph} + j_{01} * \left(e^{\frac{U-j(U)*R_S}{n_1*k_B*T}} - 1 \right) + j_{02} * \left(e^{\frac{U-j(U)*R_S}{n_2*k_B*T}} - 1 \right) + \frac{U-j(U)*R_S}{R_p} \qquad (1)$$

As a reference, we assumed a state of the art industrial solar cell with an efficiency of 19.2% [4]. This can e.g. be achieved by using selective emitter technology and a properly optimized screen printing technique with full area Al-BSF (Back Surface Field). The 90 µm wide fingers have a low line resistance of 0.22 Ω/cm, the specific contact resistance is 1.5 mΩcm^2. For the simulation we set the parameters necessary for equation (1) as n_1= 1, n_2= 2, j_{01}= 538 fA/cm^2, j_{02}= 17 nA/cm^2, R_p= 10000 Ωcm^2, j_{ph}= 40.5 mA/cm^2 at a temperature of 25°C, representing a monocrystalline 6 inch Czochralski wafer of 200 µm thickness with a resistivity of 2 Ωcm, alkaline textured, plasma-enhanced chemical vapor deposition SiN_x coating and a 80/50 Ω/sq selectively etched back emitter. The finger spacing was set to 2.1 mm. The assumed busbar width is 1.5 mm. For the contribution of the series resistance one has to add all components of a solar cell as described in [5].

To simulate the series resistance of the Al back contact we solved a partial differential equation of Poisson form assuming a continuous Ag/Al pad of 1.5 mm width on the rear side and an Al layer with a sheet resistance of 6.3 mΩ/sq. This was done by 3D simulation using the program FlexPDE 6 [6]. The width of the Al/Ag pads at the rear side for the wire design was assumed to be similar to the wire diameters. Line and contact resistance for the screen printed metal fingers were determined by four point probe measurements of comparable solar cells [7]. The ribbon/wire extension to the adjacent solar cell is assumed to be 2 mm. For a sheet resistance of 80 Ω/sq the optimal finger spacing and the number of Cu wires was determined by simulation. For the interconnected case a further R_s contribution for the tabbing, the extension and the Al rear side was added to the simulation. An additional reduction of V_{oc} caused by the Al/Ag pads was not taken into account. Also a continuous solder contact for the busbars/fingers and Al/Ag was assumed. The two-diode model describes a homogeneous solar cell without finger interruptions or variations in sheet resistivity. Additionally, a change of R_s under illumination has to be taken into account. Especially for solar cells with high series resistance this is not negligible [8, 9]. An additional absorption caused by the EVA (Ethylene Vinyl Acetate) foil [10] is also not implemented in the simulation. Optical effects like back reflection from the module glass or the busbars/wires were not taken into account. Nevertheless, this effect is relevant for the wire cell due to the round shape of the wires.

In the first simulation, a finger spacing optimization was performed and compared for the two different front grid designs: a state of the art selective emitter solar cell with either three busbars or a

multi busbar cell design assuming standard test conditions (1 sun at AM 1.5). 15 contact pins on each busbar have been considered, not leading to additional shading, and for the multi busbar design the current was collected on both ends of the wires at the edges of the solar cell. The rear side of the solar cells was set to zero potential. In the next step, the comparison of the efficiencies for the interconnected solar cell types was carried out by varying the thickness of the wires/ribbons. Therefore, an optimization for each thickness/diameter was performed, taking into account the optimal finger distance and in addition for the wire design the optimized number of wires.

For the second simulation the demand of Ag needed for a sufficient conductivity for each solar cell design was investigated. The front metallization changed from a screen printed Ag paste to a seed and plate approach [11]. Hereby a two layer metal system grants high conductivity. The conductive abilities of the seed layer were ignored, because these layers are commonly shallow. For the simulation we assumed a 40 µm wide seed layer. The shape of the plated finger was simulated as a rectangle of 40 µm width and a quarter of a circle on each side of that rectangle [12]. The dimension of the Cu ribbon was 1.5 mm x 150 µm. The diameter of the round Cu wire was set to 250 µm. An optimization was performed regarding the height of the fingers, the finger spacing and the number of wires. Hereby the assumption was made that a height increase of 1 µm by plating results in a broadening of the metal finger of 2 µm.

3. Results

The two-diode model simulation generated the IV parameters presented in Tab. 1. It can clearly be seen that the simulated values coincide with the measured IV parameters of the reference.

Table 1. IV parameters of the reference and the simulated selective emitter solar cell with three busbars

	j_{sc} [mA/cm^2]	V_{oc} [mV]	FF [%]	Eta [%]
Reference	37.63	638.7	79.78	19.17
Simulation	37.67	638.7	79.62	19.16

The contributions to the lumped series resistance are displayed in Tab. 2 for a selective emitter and full Al-BSF solar cell with either three busbar or a multi busbar design with seven wires of 250 µm diameter. The series resistance contribution of the busbar for the wire solar cell is more than 15 times higher compared to the three busbar solar cell. This effect can be explained by the measuring techniques. While the busbars are contacted with 15 pins each for the three busbar design, the current of the wire solar cell is only collected at the ends of the wires at the two edges of the solar cell.

Table 2. Contributions to the total lumped series resistance of a simulated, illuminated, selective emitter solar cell with three busbars or seven wires

		Metal back	Base	Emitter	Contact Res.	Finger	Busbar	Total
3 busbars	[mΩcm^2]	0.0036	40	246	37	98	11	433
7 wires	[mΩcm^2]	0.0036	40	246	37	19	156	497

One should note that the series resistance contribution of the emitter and the base have to be considered under illuminated conditions and therefore cannot be extracted from a dark IV measurement [9]. The reduction of series resistance was taken into account for the emitter structure and was neglected for the base. An additional reduction of series resistance has to be considered because of the selective

emitter structure. A plateau for the highly doped region leads to an additional reduction of the series resistance contribution of the emitter.

The results of the first simulation are presented in Fig. 1. In the left graph the efficiency is plotted over the finger spacing. The multi busbar cell design shows higher efficiencies, the optimum of finger spacing is almost identical and has a wide maximum at about 2 mm for both cell designs. The optimized number of wires was seven for a wire diameter of 250 µm. The IV parameters of the maximum efficiencies are presented in Tab. 3.

Table 3. IV parameters of the best three busbar and seven wire solar cell

	j_{sc} [mA/cm^2]	V_{oc} [mV]	FF [%]	Eta [%]
3 busbars	37.67	638.7	79.62	19.16
7 wires	38.46	639.3	79.11	19.45

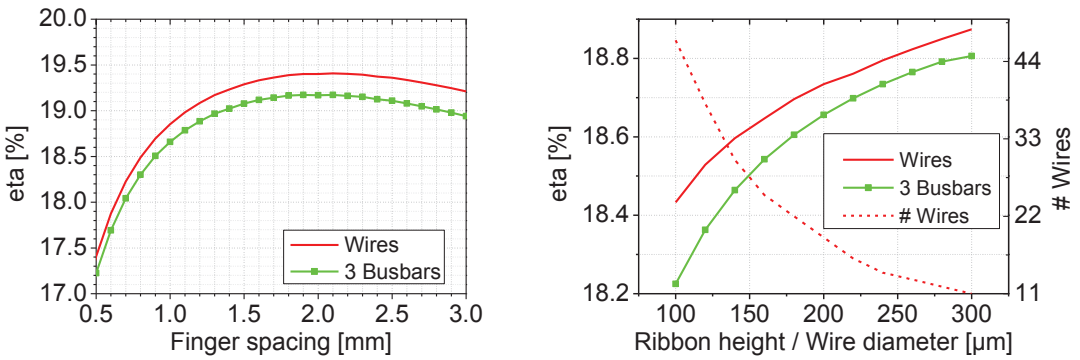

Fig. 1. Left: Efficiency of wire and three busbar solar cell over finger spacing. Right: Interconnected solar cells. The efficiency rises and the number of wires decreases for larger diameters

When interconnecting the solar cells, one has to take into account an additional series resistance due to the tabbing, the extension and the interconnected rear side. The additional series resistance contributions for a three busbar solar cell with a 150 µm high ribbon and a multi busbar solar cell with a 250 µm wire diameter are listed in Tab. 4. The contribution of the tabbing for the multi busbar design is zero because it is included in the busbar part for the multi busbar design, the busbar/wire contribution rises from 156 mΩcm^2 up to 312 mΩcm^2. Note that in the interconnected case the current is collected only on one edge of the solar cell and therefore the contribution of the series resistance rises. Therefore, the optimum number of wires increases from seven to 14 wires for the interconnected case.

Table 4. Additional series resistance contributions of a three busbar and a multi busbar solar cell interconnected as well as total lumped series resistance

		Tabbing	Extension	Metal back	Total
3 busbars	[mΩcm^2]	308	12	231	974
14 wires	[mΩcm^2]	---	12	171	809

Overall the lumped series resistance of the multi busbar solar cell design is lower and therefore the efficiency is higher. In addition the wire cell shows less shading due to the cell design. This results in a slightly higher j_{sc} value. The calculated IV parameters of both cell designs are presented in Tab. 5.

In the right graph of Fig. 1, the efficiency over ribbon height / wire diameter is plotted for the interconnected solar cell, also showing the optimal number of wires for each diameter. With increased wire diameter the number of wires decreases. This can be explained by a reduction of series resistance for increasing wire diameter on the one hand and a reduction of j_{sc} with increased shading of the wire area on the other. The multi busbar design shows higher efficiencies for all diameters.

Table 5. IV characteristics of both solar cell designs

	j_{sc} [mA/cm^2]	V_{oc} [mV]	FF [%]	Eta [%]
3 busbars	37.63	638.7	76.8	18.48
14 wires	37.93	638.9	77.64	18.82

In Fig. 2 one can observe a second beneficial effect of the multi busbar design, a significant reduction of silver needed for finger metallization with a simultaneous rise in efficiency. This can be realized by changing from screen printing to a seed and plate approach where a shallow seed layer is strengthened by plating. The rise in efficiency can be explained by a smaller effective finger length of the solar cell. For the multi busbar design the effective finger length varies from 1.6 mm to 7.1 mm for 47 to 11 wires in contrast to an effective finger length of about 25 mm for a three busbar solar cell design. The optimal amount of wires changes from 14 to 15 wires for the narrow, plated fingers.

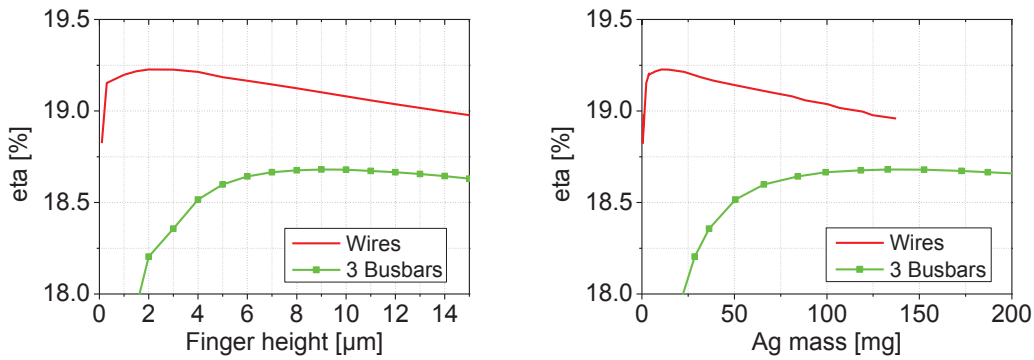

Fig. 2. Seed and plate approach (interconnected). Left: Efficiency over finger height. Right: Efficiency over silver consumption

In addition the reduced amount of Ag leads to less shading of the front grid which results in higher currents of the solar cell. Tab. 6 represents the highest theoretical efficiencies for the two cell designs assuming a ribbon height of 150 µm and a wire diameter of 250 µm.

Table 6. IV parameters for the maximum efficiencies of both cell designs using the seed and plate approach (interconnected)

	j_{sc} [mA/cm^2]	V_{oc} [mV]	FF [%]	Eta [%]
3 busbars	37.77	638.5	77.46	18.68
15 wires	38.31	638.9	78.56	19.23

The ideal amount of Ag needed for a three busbar solar cell is determined with 133 mg which results in 56 µm wide and 8 µm high fingers, assuming a 40 µm wide seed layer and a finger spacing of 1.5 mm. For the multi busbar design the optimum lies at approx 15 mg resulting in 44 µm wide and 2 µm high fingers with a finger spacing of 1.5 mm. This reduces the Ag consumed by 118 mg or 89%, and can

therefore lead to significant cost reductions. In addition, the efficiency of the interconnected wire solar cell is 0.5%$_{abs}$ higher compared to an interconnected three busbar solar cell.

One aspect that was not taken into account for the simulation is the effective shading of the wires. The effective shading of the wires has to be calculated by ray tracing simulation but first approximations show very promising results. The effective shading of a wire is much lower because perpendicularly incidenting beams will be reflected on the wire and will to a certain extent hit the wafer surface, whereas nearly all perpendicularly incidenting beams descending on a rectangular busbar tabbing with rounded edges will not get in contact with the wafer surface. Both cases can be seen in Fig. 3. For a round wire there are three regions of importance. In region (a) the beam is directly reflected onto the surface of the cell. Therefore, the effective shaded area is reduced to 70.1% of the actual area. In region (b) the reflected rays from the wire are totally reflected at the module glass. Assuming a refraction index of 1.5 for the module glass the effective shading area is reduced to 35.7%. In region (c) the reflected rays from the round wire are reflected again on the module glass but now the incident angle is larger than the angle of total reflection, therefore the beam is divided into a reflected and a transmitted part. This will also decrease the effective shaded area of the wire and lead to higher short-circuit currents.

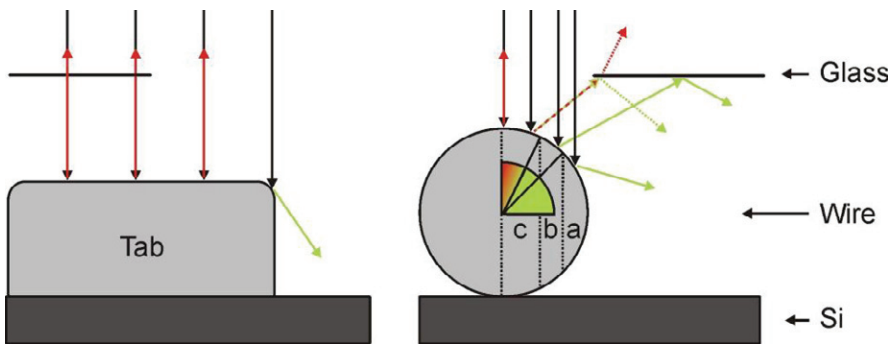

Fig. 3. Rays descending on a busbar tabbing (left) and on a round wire (right).The wire can be divided into three regions. Black arrows indicate the descending rays, green rays will reach the surface of the cell and red rays will not reach the surface

14 wires with diameter of 250 µm have a shading area of 2.24% assuming a full square wafer. But the effective shading of the wires under a module glass with refraction index 1.5 is lower than 0.8%. This will lead to an increase in j_{sc} of more than 0.6 mA/cm^2. On plated fingers one can also investigate this phenomenon.

4. Conclusion

It was demonstrated that the efficiency of a solar cell should be examined under interconnected conditions to reveal the full potential of the cell concept. Under those conditions the multi busbar design demonstrates its advantages compared to a state of the art three busbar cell design.

The multi busbar grid geometry increases the efficiency of solar cells incorporated in a module by 0.5%$_{abs}$. In addition, the multi busbar cell concept can significantly save expensive Ag per cell.

Another beneficial effect of the multi busbar concept is the geometry of the wires. By using round wires additional sunlight can enter the semiconductor because of a reflection on the wire and module glass. This will lead to even higher currents and efficiencies of this cell design. These effects were not taken into account in the simulation and may be a starting point for further investigation**s.**

Acknowledgements

The authors would kindly like to thank Gebr. Schmid GmbH for funding, especially Dirk Habermann, Helge Haverkamp, Robin Nissler and Christoph Poenisch for their support. The financial support for parts of this work by the German BMU under contracts FKZ 325168 and 0325079 is gratefully acknowledged.

References

[1] Schneider A, Rubin L, Rubin G. Solar cell improvement by new metallization techniques - The DAY4™ electrode concept. Proc. *4th WC PEC,* Waikoloa 2006, p. 1095-8

[2] Kulushich G, Zapf-Gottwick R, Mühlbauer M, Nguyen VX, Werner JH. Advanced solar cell front grid optimization. *Proc. 24th EU PVSEC*, Hamburg 2009, p. 2237-41.

[3] Chan DSH, Phang JCH. Analytical methods for the extraction of solar-cell single- and double-diode model parameters from I-V characteristics. *IEEE Trans Electron Dev* 1987;**34**:286-93.

[4] Tjahjono B, Haverkamp H, Wu V, Anditsch HT, Jung WH, Cheng J, et al. Optimizing selective emitter technology in one year of full scale production. *Proc. 26th EU PVSEC*, Hamburg 2011, p. 901-5

[5] Mette A. *New concepts for front side metallization of industrial silicon solar cells*. 2007, Dissertation University of Freiburg

[6] FlexPDE, PDE Solutions, http://www.pdesolutions.com

[7] Schroder DK. Semiconductor materials and device characterization. 3rd ed. Hoboken, New Jersey: Wiley; 1979.

[8] Aberle AG. Wenham SR, Green MA. A new method for accurate measurement of the lumped series resistance of solar cells. *Proc. 23th IEEE PVSC*, Louisville 1993, p. 133-9

[9] Fong K, McIntosh K, Blakers AW. Accurate series resistance measurement of solar cells. *Progr Photovolt Res Appl* 2011;DOI: 10.1002/pip.1216

[10] Ohl S, Hahn G. Increased internal quantum efficiency of encapsulated solar cells by using two-component silicone as encapsulant material. *Proc. 23th EU PVSEC*, Valencia 2008, p. 2693-7

[11] Glunz SW, Aleman M, Bartsch J, Bay N, Bayer K, Bergander R, et al. Progress in advanced metallization technology at Fraunhofer ISE. *Proc. 33th IEEE PVSC*, San Diego 2008, p. 399-402

[12] Kray D, Bay N, Cimiotti G, Fritz N, Glatthaar M, Kleinschmidt S, et al. Reducing Ag cost and increasing efficiency multicrystalline silicon solar cells with direct plated contacts exceeding 17% efficiency. *Proc. 26th EU PVSEC*, Hamburg 2011, p. 1199-1202